

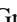
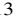
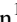


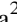



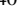





The Search for Neutrinos from TXS 0506+056 with the ANTARES Telescope

A. Albert¹, M. André², M. Anghinolfi³, G. Anton⁴, M. Ardid⁵, J.-J. Aubert⁶, J. Aublin⁷, T. Avgitas⁷, B. Baret⁷ , J. Barrios-Martí⁸, S. Basa⁹, B. Belhorma¹⁰, V. Bertin⁶, S. Biagi¹¹, R. Bormuth^{12,13}, J. Boumaaza¹⁴, S. Bourret⁷, M. C. Bouwhuis¹², H. Brânzaș¹⁵, R. Bruijn^{12,16}, J. Brunner⁶, J. Bustó⁶, A. Capone^{17,18}, L. Caramete¹⁵, J. Carr⁶ , S. Celli^{17,18,19}, M. Chabab²⁰, R. Cherkaoui El Moursli¹⁴, T. Chiarusi²¹, M. Circella²², J. A. B. Coelho⁷, A. Coleiro^{7,8}, M. Colomer^{7,8}, R. Coniglione¹¹, H. Costantini⁶, P. Coyle⁶, A. Creusot⁷, A. F. Díaz²³, A. Deschamps²⁴, C. Distefano¹¹, I. Di Palma^{17,18}, A. Domi^{3,25}, R. Donà^{21,26}, C. Donzaud^{7,27}, D. Dornic⁶, D. Drouhin¹, T. Eberl²⁸, I. El Bojaddaini²⁹, N. El Khayati¹⁴, D. Elsässer³⁰, A. Enzenhöfer^{6,28}, A. Ettahiri¹⁴, F. Fassi¹⁴, I. Felis⁵, P. Fermani^{17,18}, G. Ferrara¹¹, L. Fusco⁷ , P. Gay^{7,31}, H. Glotin³², T. Grégoire⁷, R. Gracia Ruiz¹, K. Graf²⁸, S. Hallmann²⁸, H. van Haren³³, A. J. Heijboer¹², Y. Hello²⁴, J. J. Hernández-Rey⁸, J. Höfl²⁸, J. Hofestädt²⁸, G. Illuminati⁸, M. de Jong^{12,13}, M. Jongen¹², M. Kadler³⁰ , O. Kalekin²⁸ , U. Katz²⁸ , N. R. Khan-Chowdhury⁸, A. Kouchner^{7,34}, M. Kreter³⁰, I. Kreykenbohm³⁵, V. Kulikovskiy^{3,36}, C. Lachaud⁷, R. Lahmann²⁸, D. Lefèvre^{37,38}, E. Leonora³⁹ , M. Lotze⁸, S. Loucatos^{7,40}, M. Marcelin⁹, A. Margiotta^{21,26}, A. Marinelli^{41,42} , J. A. Martínez-Mora⁵, R. Mele^{43,44} , K. Melis^{12,45}, P. Migliozzi⁴³, A. Moussa²⁹, S. Navas⁴⁶, E. Nezri⁹, A. Nuñez^{6,9}, M. Organokov¹, G. E. Pávlaș¹⁵, C. Pellegrino^{21,26}, P. Piattelli¹¹, V. Popa¹⁵, T. Pradier¹, L. Quinn⁶, C. Racca⁴⁷, N. Randazzo³⁹, G. Riccobene¹¹, A. Sánchez-Losa²², M. Saldaña⁵, I. Salvadori⁶, D. F. E. Samtleben^{12,13}, M. Sanguineti^{3,25} , P. Sapienza¹¹, F. Schüssler⁴⁰, M. Spurio^{21,26} , Th. Stolarczyk⁴⁰ , M. Taiuti^{3,25}, Y. Tayalati¹⁴, A. Trovato¹¹, B. Vallage^{7,40}, V. Van Elewyck^{7,34}, F. Versari^{21,26}, D. Vivolo^{43,44}, J. Wilms³⁵ , D. Zaborov⁶, J. D. Zornoza⁸, and J. Zúñiga⁸

(ANTARES Collaboration)

¹ Université de Strasbourg, CNRS, IPHC UMR 7178, F-67000 Strasbourg, France; antares.spokesperson@in2p3.fr

² Technical University of Catalonia, Laboratory of Applied Bioacoustics, Rambla Exposició, E-08800 Vilanova i la Geltrú, Barcelona, Spain

³ INFN—Sezione di Genova, Via Dodecaneso 33, I-16146 Genova, Italy

⁴ Erlangen Centre for Astroparticle Physics, Friedrich-Alexander-Universität Erlangen-Nürnberg, D-91058 Erlangen, Germany

⁵ Institut d'Investigació per a la Gestió Integrada de les Zones Costaneres (IGIC)—Universitat Politècnica de València. C/Paranimf 1, E-46730 Gandia, Spain

⁶ Aix Marseille Univ, CNRS/IN2P3, CPPM, Marseille, France

⁷ APC, Univ Paris Diderot, CNRS/IN2P3, CEA/Irfu, Obs de Paris, Sorbonne Paris Cité, France

⁸ IFIC—Instituto de Física Corpuscular (CSIC—Universitat de València) c/Catedrático José Beltrán, 2 E-46980 Paterna, Valencia, Spain

⁹ LAM—Laboratoire d'Astrophysique de Marseille, Pôle de l'Étoile Site de Château-Gombert, rue Frédéric Joliot-Curie 38, F-13388 Marseille Cedex 13, France

¹⁰ National Center for Energy Sciences and Nuclear Techniques, B.P.1382, R.P.10001 Rabat, Morocco

¹¹ INFN—Laboratori Nazionali del Sud (LNS), Via S. Sofia 62, I-95123 Catania, Italy

¹² Nikhef, Science Park, Amsterdam, The Netherlands

¹³ Huygens-Kamerlingh Onnes Laboratorium, Universiteit Leiden, The Netherlands

¹⁴ University Mohammed V in Rabat, Faculty of Sciences, 4 av. Ibn Battouta, B.P. 1014, R.P. 10000 Rabat, Morocco

¹⁵ Institute of Space Science, RO-077125 Bucharest, Măgurele, Romania

¹⁶ Universiteit van Amsterdam, Instituut voor Hoge-Energie Fysica, Science Park 05, 1098 XG Amsterdam, The Netherlands

¹⁷ INFN—Sezione di Roma, P.le Aldo Moro 2, I-00185 Roma, Italy

¹⁸ Dipartimento di Fisica dell'Università La Sapienza, P.le Aldo Moro 2, I-00185 Roma, Italy

¹⁹ Gran Sasso Science Institute, Viale Francesco Crispi 7, I-00167 L'Aquila, Italy

²⁰ LPHEA, Faculty of Science—Semlali, Cadi Ayyad University, P.O.B. 2390, Marrakech, Morocco

²¹ INFN—Sezione di Bologna, Viale Berti-Pichat 6/2, I-40127 Bologna, Italy

²² INFN—Sezione di Bari, Via E. Orabona 4, I-70126 Bari, Italy

²³ Department of Computer Architecture and Technology/CITIC, University of Granada, E-18071 Granada, Spain

²⁴ Géoazur, UCA, CNRS, IRD, Observatoire de la Côte d'Azur, Sophia Antipolis, France

²⁵ Dipartimento di Fisica dell'Università, Via Dodecaneso 33, I-16146 Genova, Italy

²⁶ Dipartimento di Fisica e Astronomia dell'Università, Viale Berti Pichat 6/2, I-40127 Bologna, Italy

²⁷ Université Paris-Sud, F-91405 Orsay Cedex, France

²⁸ Friedrich-Alexander-Universität Erlangen-Nürnberg, Erlangen Centre for Astroparticle Physics, Erwin-Rommel-Str. 1, D-91058 Erlangen, Germany

²⁹ University Mohammed I, Laboratory of Physics of Matter and Radiations, B.P.717, Oujda 6000, Morocco

³⁰ Institut für Theoretische Physik und Astrophysik, Universität Würzburg, Emil-Fischer Str. 31, D-97074 Würzburg, Germany

³¹ Laboratoire de Physique Corpusculaire, Clermont Université, Université Blaise Pascal, CNRS/IN2P3, BP 10448, F-63000 Clermont-Ferrand, France

³² LIS, UMR Université de Toulon, Aix Marseille Université, CNRS, F-83041 Toulon, France

³³ Royal Netherlands Institute for Sea Research (NIOZ) and Utrecht University, Landsdiep 4, 1797 SZ 't Horntje (Texel), The Netherlands

³⁴ Institut Universitaire de France, F-75005 Paris, France

³⁵ Dr. Reimei-Sternwarte and ECAP, Friedrich-Alexander-Universität Erlangen-Nürnberg, Sternwartstr. 7, D-96049 Bamberg, Germany

³⁶ Moscow State University, Skobeltsyn Institute of Nuclear Physics, Leninskie gory, 119991 Moscow, Russia

³⁷ Mediterranean Institute of Oceanography (MIO), Aix-Marseille University, F-13288, Marseille, Cedex 9, France

³⁸ Université du Sud Toulon-Var, CNRS-INSU/IRD UM 110, F-83957, La Garde Cedex, France

³⁹ INFN—Sezione di Catania, Via S. Sofia 64, I-95123 Catania, Italy

⁴⁰ IRFU, CEA, Université Paris-Saclay, F-91191 Gif-sur-Yvette, France

⁴¹ INFN—Sezione di Pisa, Largo B. Pontecorvo 3, I-56127 Pisa, Italy

⁴² Dipartimento di Fisica dell'Università, Largo B. Pontecorvo 3, I-56127 Pisa, Italy

⁴³ INFN—Sezione di Napoli, Via Cintia I-80126 Napoli, Italy

⁴⁴ Dipartimento di Fisica dell'Università Federico II di Napoli, Via Cintia I-80126, Napoli, Italy

⁴⁵ Universiteit van Amsterdam, Instituut voor Hoge-Energie Fysica, Science Park 105, 1098 XG Amsterdam, The Netherlands

⁴⁶ Dpto. de Física Teórica y del Cosmos & C.A.F.P.E., University of Granada, E-18071 Granada, Spain⁴⁷ GRPHE—Université de Haute Alsace—Institut universitaire de technologie de Colmar, 34 rue du Grillenbreit BP 50568-68008 Colmar, France
Received 2018 July 10; revised 2018 August 3; accepted 2018 August 5; published 2018 August 17

Abstract

The results of three different searches for neutrino candidates, associated with the IceCube-170922A event or from the direction of TXS 0506+056, by the ANTARES neutrino telescope, are presented. The first search refers to the online follow-up of the IceCube alert; the second is based on the standard time-integrated method employed by the Collaboration to search for point-like neutrino sources; the third uses information from the IceCube time-dependent analysis that reported bursting activity centered on 2014 December 13, as input for an ANTARES time-dependent analysis. The online follow-up and the time-dependent analysis yield no events related to the source. The time-integrated study performed over a period from 2007 to 2017 fits 1.03 signal events, which corresponds to a p -value of 3.4% (not considering trial factors). Only for two other astrophysical objects in our candidate list has a smaller p -value been found. When considering that 107 sources have been investigated, the post-trial p -value for TXS 0506+056 corresponds to 87%.

Key words: astroparticle physics – elementary particles – galaxies: active

1. Introduction

High-energy (HE) neutrinos are produced through the decay of charged mesons, and are associated with γ -rays produced by the decay of neutral mesons. These mesons were previously produced in the interactions of protons or nuclei with ambient matter or radiation. Thus, the observation of neutrinos associated with known sources of γ -rays and/or electromagnetic radiation provide identifications of cosmic objects where hadrons are accelerated.

The IceCube Collaboration has reported a significant excess of a diffuse flux of HE astrophysical neutrinos over the atmospheric background (Aartsen et al. 2014, 2016). However, no individual HE neutrino source has been identified so far. A recent HE neutrino detected by the IceCube experiment was connected with observations in γ -rays and at other wavelengths of the electromagnetic spectrum from blazar TXS 0506+056 (IceCube Collaboration et al. 2018). This may indicate that this blazar (a BL Lac object, at redshift $z = 0.3365 \pm 0.0010$ Paiano et al. 2018) is an individually identifiable source of HE neutrinos. Two independent analyses (one time-integrated and one time-dependent) of IceCube data searching for neutrino emission at the position of the blazar confirmed an excess of events at the level of 3.5σ (Aartsen et al. 2018).

The ANTARES (Ageron et al. 2011) telescope is a deep-sea Cherenkov neutrino detector, located 40 km off shore from Toulon, France, in the Mediterranean Sea. The telescope aims primarily to detect the neutrino-induced muons that cause the emission of Cherenkov light in the detector (track-like events). Charged current interactions induced by electron neutrinos (and, possibly, by tau neutrinos of cosmic origin), or neutral current interactions of all neutrino flavors, can be reconstructed as shower-like events (Albert et al. 2017b). Due to its location, the ANTARES detector mainly observes the Southern sky (2π sr at any time). Events arising from sky positions in the decl. band $-90^\circ \leq \delta \leq -48^\circ$ are always visible as upgoing. Neutrino-induced events in the decl. band $-48^\circ \leq \delta \leq +48^\circ$ are visible as upgoing, with a fraction of time decreasing from 100% down to 0%.

In this document, the results of three different searches by the ANTARES neutrino telescope for neutrino candidates, associated with the IceCube-170922A event or from the direction of TXS 0506+056, are presented. The first search refers to the online follow-up associated with IceCube-170922A (Section 2). The second is based on the standard

likelihood method employed by the Collaboration to search for point-like neutrino sources (Section 3). The third uses the information from the time-dependent analysis performed by the IceCube Collaboration (Aartsen et al. 2018), which reported bursting activity centered on 2014 December 13, as input for an ANTARES time-dependent analysis. Conclusions are reported in Section 5.

2. Online Searches for Neutrinos in ANTARES Associated with IceCube-170922A EHE

Following the IceCube observation of a HE neutrino candidate event, IceCube-170922A, which occurred at $T_0 = 17/09/22, 20:54:30.43$ UT (in the following referred to as IC170922A), the ANTARES Collaboration performed an online follow-up analysis to look for additional neutrinos from the reported event direction.

The IceCube event was identified by the extremely high-energy (EHE) track event selection and reported with a GCN circular (IceCube Collaboration 2017). This EHE event had a high probability of being of astrophysical origin and the IceCube Collaboration encouraged follow-up to help with identifying a possible astrophysical source. The reported position (J2000, with 90% point-spread function (PSF) containment) was R.A. = $77^{\circ}43^{+1^{\circ}30}_{-0^{\circ}30}$ and $\delta = 5^{\circ}72^{+0^{\circ}70}_{-0^{\circ}40}$.

The reconstructed direction of IC170922A corresponded, at the location of the ANTARES detector, to a direction $14^{\circ}2$ below the horizon, Figure 1. A possible neutrino candidate would thus be detected as an upgoing event.

Based on the originally communicated location of IC170922A, HE neutrino candidates were searched for in the ANTARES online data stream, relying on a fast algorithm that selects only upgoing neutrino track candidates (Adrián-Martínez et al. 2016b). This algorithm uses an idealized detector geometry and so far has no information on the dynamical positioning calibration. At 10 TeV, the median angular resolution for muon neutrinos is below $0^{\circ}5$. For neutrino energies below ~ 100 TeV, ANTARES has a competitive sensitivity to this position in the sky.

As a result of this search, no upgoing muon neutrino candidate event was recorded in a cone of 3° centered on the IceCube event coordinates and within a ± 1 hr time window centered on the event time. A search over an extended time window of ± 1 day also yielded no detection. Averaged over a day, the source is below the ANTARES horizon, with a 46%

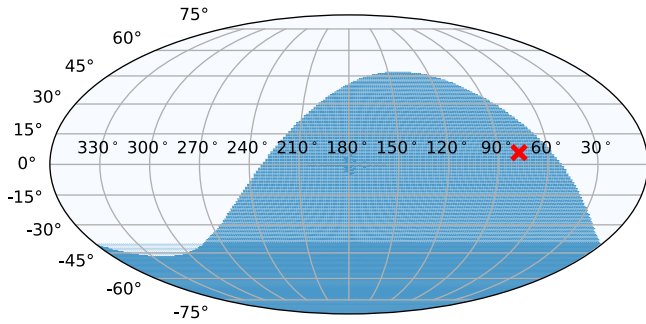


Figure 1. Visibility map for the ANTARES detector of IC170922A (represented by the red marker) in equatorial coordinates. The sky regions below and above the horizon at the alert time are shown in blue and white, respectively. Events that originate from the blue (white) region will be seen as upgoing (downgoing) in the detector frame.

fraction. The result of this study was reported in ANTARES Collaboration (2017).

This non-detection in 2 hr was used to provide a preliminary constraint on the neutrino fluence, computed following Adrián-Martínez et al. (2016a). A point source of neutrinos, with a power-law spectrum $\frac{dN}{dE} \propto E^{-\gamma}$, has been assumed. For a flux with $\gamma = 2.0$, the 90% C.L. fluence upper limit is 15 GeV cm^{-2} , integrated over the energy range 3.3 TeV–3.4 PeV (the range corresponding to 5%–95% of the detectable flux). For $\gamma = 2.5$, the 90% C.L. fluence upper limit is 34 GeV cm^{-2} , integrated in the 450 GeV–280 TeV energy range.

3. Time-integrated Search for Neutrinos from TXS 0506+056

After the IceCube alert, the Fermi-LAT Collaboration announced that the blazar TXS 0506+056, located at 6 arcmin from the center of the estimated IC170922A direction, showed enhanced gamma-ray activity during the week of the alert (ATel #10791). Then, the MAGIC Collaboration observed this source under good weather conditions and a 5σ detection above 100 GeV was achieved after 12 hr of observations from September 28 till October 3 (ATel #10817). Other γ -ray ground detectors, namely the H.E.S.S. (ATel #10787), HAWC (ATel #10802) and VERITAS (ATel #10833) Collaborations, reported no significant detection.

Considering the potential association between IC170922A and the blazar TXS 0506+056, its location was scrutinized following the ANTARES standard point-source method. In this approach, the directions of a predefined list of neutrino source candidates are investigated to look for an excess of events and to determine a flux upper limit in case of a null observation. The results of this study using 106 pre-selected sources (not including TXS 0506+056) have been recently published (Albert et al. 2017a). The data were recorded from 2007 January 29, to 2015 December 31, corresponding to a livetime of 2424 days.

The neutrino event selection is optimized following a blinding procedure on pseudodata sets randomized in time before performing the analysis. To find clusters of neutrinos from cosmic sources, a maximum likelihood ratio approach is followed. While atmospheric neutrino events are randomly distributed, neutrinos from point-like sources are expected to accumulate in spatial clusters. The likelihood describes the data in terms of signal and background probability density functions

that include both shower-like and track-like events. The signal likelihood includes a parameterization of the PSF and of the probability density function of the reconstructed energy, which is estimated for each event.

The PSF is defined as the probability density of finding a reconstructed event at an angular distance $\Delta\Psi$ around the direction of the source. It depends on the angular resolution of the event sample. The PSFs (for track- and shower-like events) are determined from Monte Carlo simulations of neutrinos with an E^{-2} energy spectrum: about 50% of the track (shower) events are reconstructed within 0.4 (3°) from the parent neutrino.

The probability density functions for the energy estimators take into account the different energy spectra of atmospheric and cosmic neutrinos. The spectrum of both is expected to follow a power-law type, $\propto E^{-\gamma}$, but with different values for the spectral indexes: $\gamma \simeq 3.6$ for atmospheric neutrinos (Adrián-Martínez et al. 2013) and $\gamma \simeq 2.0$ for cosmic neutrinos. Thus, the flux of cosmic neutrinos is expected to exceed the atmospheric neutrino flux above a certain energy threshold, estimated around 100 TeV.

The background rate depends on the decl., δ . Given the expected small contribution of a cosmic signal in the overall data set, the background rate is estimated directly from the data. Due to the Earth's rotation and a sufficiently uniform exposure, the background is considered independent of R.A. The expected number of background events at the decl. of IC170922A in the livetime of 2424 days is $0.18/\text{deg}^2$ and $4 \times 10^{-3}/\text{deg}^2$ for track-like and shower-like events, respectively.

The blazar TXS 0506+056 was added to the list of 106 already studied objects, and analyzed without changing the predefined conditions. The corresponding number of signal events, μ_{sig} , which fits the likelihood signal function for this source, is $\mu_{\text{sig}} = 1.03$. This signal likelihood of μ_{sig} corresponds to a pre-trial p -value of 2.6% to be compatible with the background-only hypothesis. By referring to the candidate list of Table 3 of Albert et al. (2017a), only for the directions of two other objects, a smaller p -value had been evaluated: HESSJ0632+057, with a pre-trial p -value of 0.16%, and PKS1440-389, with a pre-trial p -value of 0.5%. After TXS 0506+056, the fourth position corresponds to PKS0235+164, with 5%. When considering that 107 sources have been investigated, the post-trial p -value for TXS 0506+056 is 87%.

There is one track-like event that mostly influences the fit (see Figure 2) whose position is within 1σ from the source position. This event occurred on 2013 December 12 (MJD: 56638.70832).

Fully calibrated data collected by the ANTARES detector during 2016 and 2017 are available. Limited to the TXS 0506+056 source, these additional two years of data have been unblinded using the same predefined conditions used for the 2007–2015 period. The additional livetime corresponds to 712 days. In this additional sample, there are two new tracks within 5° from the source.

The information concerning the 13 track-like and 1 shower-like neutrino candidates in the period 2007–2017 with coordinates within 5° from TXS 0506+056 are reported in Table 1. Within a radius of 5° in a livetime of 3136 days, 17 ± 4 atmospheric neutrino events are expected. The amount of detected light can be used to infer the energy of the event. This information can be subsequently used to estimate the

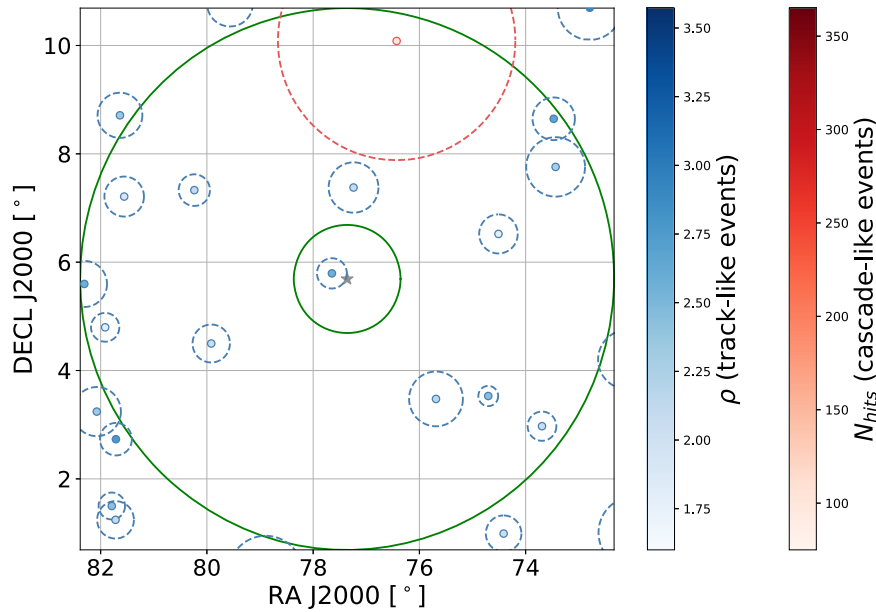


Figure 2. Distribution of ANTARES events in the (R.A., δ) coordinates around the position of TXS 0506+056. The inner (outer) green line depicts the one (five) degree distance from the source position, indicated as a gray star. The red point denotes a shower-like event, whereas the blue points indicate track-like events. The dashed circles around the events indicate the angular error estimate. The different shades of red and blue correspond to the values assumed by the energy estimators, and the right legend shows the color scales. The number of hits is used for shower-like events and the ρ parameter is used for track-like events. Refer to Albert et al. (2017a) for further details on the energy estimators.

energy of the parent neutrino. However, the neutrino energy distribution is distorted by the limited energy resolution and the overall acceptance of the detector. As discussed in depth in (Adrián-Martínez et al. 2013) for the ν_μ case, the measured muon energy distribution can be translated into the neutrino energy spectrum through a response matrix determined from Monte Carlo simulations, and an unfolding procedure. The value of the energy estimator, ρ , for the closest event to TXS 0506+056 is such that only 9% of the observed muon neutrinos in the ANTARES telescope have higher energies. According to the unfolded distribution, 10% of the atmospheric neutrinos have energies larger than 6 TeV. The fraction of detected neutrinos with estimated energy larger than that observed for each event present in Table 1 is reported in the last column.

After the inclusion of the 2016–2017 data, the number of fitted signal events, μ_{sig} , remains 1.03 and the associated p -value rises from 2.6% to 3.4%. Using the total livetime of 3136 days, the corresponding 90% C.L. upper limits on the flux normalization factor at the energy of 100 TeV, $\Phi_{100 \text{ TeV}}^{90\%}$, assuming a steady neutrino source and spectral index $\gamma = 2.0$, is $1.6 \times 10^{-18} \text{ GeV}^{-1} \text{ cm}^{-2} \text{ s}^{-1}$ in the 5%–95% energy range 2 TeV–4 PeV.

This result does not appreciably change for harder spectral indexes ($1.7 \leq \gamma \leq 2.0$). For softer spectral indexes, the PSF widens; for this reason, the fitted value of μ_{sig} slightly increases, because events that have lower energy and are further away from the source also contribute to the signal. On the other hand, the p -value slightly increases, as the expected signal becomes more similar to the atmospheric background (softer spectrum, more distant events). Numerically, for $\gamma = 2.3$ (2.5) the fitted signal is $\mu_{\text{sig}} = 1.06$ (1.09), the p -value 4.2% (4.9%) and the upper limit on the normalization factor $\Phi_{100 \text{ TeV}}^{90\%} = 1.4(1.0) \times 10^{-18} \text{ GeV}^{-1} \text{ cm}^{-2} \text{ s}^{-1}$.

4. Search for Neutrinos in the Bursting Period

The time-dependent analysis performed by the IceCube Collaboration (Aartsen et al. 2018) contains a significant excess that is identified by two time-window shapes (one Gaussian-shaped and one box-shaped time profile).

The ANTARES Collaboration has developed a time-dependent analysis aimed at finding correlations between neutrinos and high-energy electromagnetic emission, reducing by a factor of 2–3 the signal required for a discovery with respect to a time-integrated search (Albert et al. 2017c). For TXS 0506+056, a search similar to that reported in ANTARES Collaboration (2015) was performed, with a bursting period as defined by the two profiles provided by the IceCube Collaboration, instead of an electromagnetic light curve.

The first one (denoted in the following as “Gaussian flare”) is modeled by a Gaussian signal centered on MJD 57004 and with a standard deviation $\sigma = 55.0$ days. We considered a period $\pm 5\sigma$ wide, corresponding to 550 flaring days. The second one (referred to as “box flare”) assumes a box-shaped flare starting at MJD 56937.81 and ending at MJD 57096.21, corresponding to 158.40 flaring days.

The time-dependent analysis first defines the values of selection cuts that, assuming a power-law neutrino spectrum for the signal, optimizes the Model Rejection Factor. Three different spectral indexes for the neutrino spectrum have been considered ($\gamma = 2.0, 2.1, \text{ and } 2.2$), and the cut parameters to be optimized are the maximum reconstructed neutrino zenith angle, θ , and the quality of reconstructed tracks, Λ . The resulting optimized set of cuts for the three considered spectral indexes are $\cos \theta > -0.15$ and $\Lambda > -5.6$. For comparison, the corresponding cuts for the time-integrated search reported in Section 3 are $\cos \theta > -0.10$ and $\Lambda > -5.2$. This means that the time-dependent analysis allows for more downward-going neutrino candidates and tracks with a lower reconstruction quality parameter; refer to Figure 2 of Albert et al. (2017a).

Table 1
Neutrino Candidates Registered by the ANTARES Detector within an Angular Distance $\Delta\Psi$ from TXS 0506+056

#	(R.A., δ) (deg)	$\Delta\Psi$ (deg)	MJD	Date (year/mm/dd)	ρ (a.u.)	$f(>\rho)$
1	(77.65, 5.79)	0.30	56638.70832	2013 Dec 12	2.58	0.09
2	(77.24, 7.38)	1.69	54601.04530	2008 May 15	2.10	0.40
3	(75.69, 3.48)	2.77	55396.03988	2010 Jul 19	2.16	0.33
4	(79.92, 4.50)	2.81	55585.28089	2011 Jan 24	2.05	0.47
5	(74.51, 6.52)	2.95	56143.90394	2012 Aug 04	1.78	0.87
6	(80.24, 7.33)	3.30	56268.37325	2012 Dec 07	2.11	0.39
7	(74.70, 3.53)	3.42	56495.86001	2013 Jul 22	2.45	0.14
8	(73.44, 7.76)	4.41	57455.29659	2016 Mar 08	2.27	0.24
9	(81.56, 7.21)	4.44	56298.41381	2013 Jan 06	1.94	0.63
10	(73.69, 2.97)	4.56	54742.73522	2008 Oct 03	2.06	0.44
11	(81.91, 4.80)	4.62	57392.49813	2016 Jan 05	1.80	0.83
12	(73.47, 8.65)	4.86	54853.53484	2009 Jan 22	2.67	0.07
13	(82.31, 5.60)	4.92	55399.13414	2010 Jul 22	2.57	0.09
S1	(76.43, 10.08)	4.49	55144.74625	2009 Nov 09	101	0.74

Note. There are 13 tracks and 1 shower event (S1). The table reports the following for each neutrino candidate: the equatorial coordinates (δ , R.A.); the angular distance $\Delta\Psi$ from TXS 0506+056; the modified Julian date (MJD); the date (year/mm/dd); the energy estimator value (arbitrary units, a.u.); and the fraction, f , of events with energy estimator values larger than that of the event. For the shower S1 the energy estimator is the number of hits used in the fit. Refer to Albert et al. (2017a) for more details. Events # 8 and 11 were recorded during the 2016–2017 period.

According to this set of cuts, the expected background during the box flare has been estimated as 0.04 (4) events within $0^\circ.5$ (5°) from the source. This is a factor ~ 4 larger than that determined for the time-integrated search. The background increases because a larger fraction of atmospheric muons is mis-reconstructed and because more low-energy atmospheric neutrinos are included. Thanks to the reduced observational time window, the method allows the presence of lower energy cosmic neutrinos and de facto corresponds to an analysis sensitive to a softer neutrino energy spectrum.

After the optimization, the data have been unblinded. The results are compatible with the expectation from the atmospheric background, and no signal has been found during either of the considered flares. Within 2° from the source, 10 background events are expected during the analyzed period, while 13 events have been found in data. None of them lie within either of the two considered flaring periods. From these null results, 90% C.L. upper limits have been derived for the neutrino flux. For an $E^{-2.0}$ ($E^{-2.1}$) [$E^{-2.2}$] spectrum they correspond to a normalization factor of $\Phi_{100\text{TeV}}^{90\%} = 4.6(4.4)[4.2] \times 10^{-18} \text{ GeV}^{-1} \text{ cm}^{-2} \text{ s}^{-1}$ for the Gaussian-shaped period. The energy range containing the 5%–95% of the detectable flux is 2.0 (1.3) [1.0] TeV–3.2 (1.6) [1.0] PeV. For the box-shaped period, the flux normalization factors are a factor of 3.3 higher.

5. Conclusions

The GCN circular (IceCube Collaboration 2017) on the EHE neutrino candidate event, IC170922A, promptly triggered a search for neutrino candidates in the ANTARES online data stream. The position of the IC170922A event at the location of the ANTARES detector is $14^\circ.2$ below the horizon. For neutrino energies below ~ 100 TeV, ANTARES has competitive sensitivity with respect to IceCube to this position in the sky. No upgoing muon neutrino candidate event was recorded within 3° around the IC170922A direction within ± 1 hr centered on the event time.




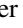
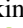

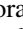


Successively, due to the potential association between IC170922A and the blazar TXS 0506+56, this source has been scrutinized following the ANTARES standard point-source method. TXS 0506+056 was not considered among the 106 pre-selected sources in our recent study (Albert et al. 2017a), and a dedicated analysis was done using two additional years of data. The considered period (from 2007 to 2017) corresponds to a total livetime of 3136 days. The result yields a number of fitted signal events $\mu_{\text{sig}} = 1.03$ with an associated pre-trial p -value of 3.4%. This is the third most significant source on our list. When considering that 107 sources have been investigated, the post-trial p -value for TXS 0506+056 corresponds to 87%.




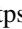
Finally, according to the results of a time-dependent analysis performed by the IceCube Collaboration (Aartsen et al. 2018), we applied our standard time-dependent analysis on a bursting period centered on MJD 57004 (2014 December 13). The analysis, which relies on relaxed selection criteria for the neutrino direction and reconstructed track quality, yielded no events within the Gaussian-shaped and the box-shaped periods defined by the IceCube analysis.

We thank the IceCube Collaboration for sharing information before the public release. The authors acknowledge the financial support of the funding agencies: Centre National de la Recherche Scientifique (CNRS), Commissariat à l'énergie atomique et aux énergies alternatives (CEA), Commission Européenne (FEDER fund and Marie Curie Program), Institut Universitaire de France (IUF), IdEx program and UnivEarthS Labex program at Sorbonne Paris Cité (ANR-10-LABX-0023 and ANR-11-IDEX-0005-02), Labex OCEVU (ANR-11-LABX-0060) and the A*MIDEX project (ANR-11-IDEX-0001-02), Région Île-de-France (DIM-ACAV), Région Alsace (contrat CPER), Région Provence-Alpes-Côte d'Azur, Département du Var and Ville de La Seyne-sur-Mer, France; Bundesministerium für Bildung und Forschung (BMBF), Germany; Istituto Nazionale di Fisica Nucleare (INFN), Italy; Nederlandse organisatie voor Wetenschappelijk Onderzoek (NWO), the Netherlands; Council of the President of the Russian Federation for young scientists

and leading scientific schools supporting grants, Russia; National Authority for Scientific Research (ANCS), Romania; Ministerio de Economía y Competitividad (MINECO): Plan Estatal de Investigación (refs. FPA2015-65150-C3-1-P, -2-P and -3-P, (MINECO/FEDER)), Severo Ochoa Centre of Excellence and MultiDark Consolider (MINECO), and Prometeo and Grisolia programs (Generalitat Valenciana), Spain; Ministry of Higher Education, Scientific Research and Professional Training, Morocco. We also acknowledge the technical support of Ifremer, AIM, and Foselev Marine for the sea operation and the CC-IN2P3 for the computing facilities.

ORCID iDs

B. Baret  <https://orcid.org/0000-0001-6064-3858>
 J. Carr  <https://orcid.org/0000-0002-6695-3977>
 L. Fusco  <https://orcid.org/0000-0001-8254-3372>
 M. Kadler  <https://orcid.org/0000-0001-5606-6154>
 O. Kalekin  <https://orcid.org/0000-0001-6206-1288>
 U. Katz  <https://orcid.org/0000-0002-7063-4418>
 E. Leonora  <https://orcid.org/0000-0002-0536-3551>
 A. Marinelli  <https://orcid.org/0000-0002-1466-1219>
 R. Mele  <https://orcid.org/0000-0002-9165-4231>

M. Sanguineti  <https://orcid.org/0000-0002-7206-2097>
 M. Spurio  <https://orcid.org/0000-0002-8698-3655>
 Th. Stolarczyk  <https://orcid.org/0000-0002-0551-7581>
 J. Wilms  <https://orcid.org/0000-0003-2065-5410>

References

- Aartsen, M. G., Abraham, K., Ackermann, M., et al. 2016, *ApJ*, 833, 3
 Aartsen, M. G., Ackermann, M., Adams, J., et al. 2014, *PhRvL*, 113, 101101
 Aartsen, M. G., Ackermann, M., Adams, J., et al. 2018, *Sci*, 361, doi:10.1126/science.aat2890
 Adrián-Martínez, S., Ageron, M., Albert, A., et al. 2016b, *JCAP*, 02, 062
 Adrián-Martínez, S., Albert, A., Al Samarai, I., et al. 2013, *EPJC*, 73, 2606
 Adrián-Martínez, S., Albert, A., André, M., et al. (ANTARES Collaboration, IceCube Collaboration, LIGO Scientific Collaboration, Virgo Collaboration) 2016a, *PhRvD*, 93, 122010
 Ageron, M., Aguilar, J. A., Al Samarai, I., et al. 2011, *NIMPA*, 656, 11
 Albert, A., André, M., Anghinolfi, M., et al. 2017a, *PhRvD*, 96, 082001
 Albert, A., André, M., Anghinolfi, M., et al. 2017b, *AJ*, 154, 275
 Albert, A., André, M., Anton, G., et al. 2017c, *JCAP*, 04, 019
 ANTARES Collaboration 2015, *JCAP*, 12, 014
 ANTARES Collaboration 2017, *ATel*, 10773, 1
 IceCube Collaboration, Aartsen, M. G., Ackermann, M., et al. 2018, *Sci*, 361, eaat1378
 IceCube Collaboration 2017, *GCN*, 21916, 1
 Paiano, S., Falomo, R., Treves, A., & Scarpa, R. 2018, *ApJL*, 854, L32